様式第１９

学 会 等 発 表 実 績

委託業務題目「新規バイオマーカーPRDM14による難治性乳がん・すい臓がんの診断法の開発」
機関名　東京大学医科学研究所
（今井浩三）

## １．学会等における口頭・ポスター発表

| 発表した成果（発表題目、口頭・ポスター発表の別） | 発表者氏名 | 発表した場所（学会等名） | 発表した時期 | 国内・外の別 |
|---|---|---|---|---|
| A combination of the anti-fibroblast growth factor receptor 1 monoclonal antibody and interferon-a/b suppreses human hepatic cancer cells in vitro and in vivo.（口頭） | Kato Y, Hiromi H, Tujisaki M, Matsune T, Sasaki S, Hinoda Y, Shinomura Y, Imai K. | 41st Congress of the International Society of Oncology and Biomarkers. 2014, Barcelona. | 2014 3月 | 国外 |
| 東京大学医科学研究所におけるTRの現状と展望　シンポジウム2「我が国におけるトランスレーショナルリサーチの現状とこれからの展望」(口頭) | 今井浩三 | 第51回日本臨床分子医学会学術集会　東京国際フォーラム | 2014年4月 | 国内 |
| 招聘講演「東大医科研における橋渡し研究とその発展」(口頭) | 今井浩三 | 第103回日本病理学会総会　広島国際会議場フェニックスホール | 2014年4月 | 国内 |
| 特別講演「最先端医療の開発とDNA情報に基づく新たな社会」(口頭) | 今井浩三 | 多摩大学 寺島実郎監修リレー講座　東京 | 2014年6月 | 国内 |
| 東京大学医科学研究所における橋渡し研究の現状とその展開(口頭) | 今井浩三 | 「ヒト疾患モデル研究センター」シンポジウム, 東京理科大学生命医科学研究所 | 2014年7月 | 国内 |

## ２．学会誌・雑誌等における論文掲載

| 掲載した論文（発表題目） | 発表者氏名 | 発表した場所（学会誌・雑誌等名） | 発表した時期 | 国内・外の別 |
|---|---|---|---|---|
| Mesenchymal stem cells cancel azoxymethane-induced tumor initiation. | Nasuno M, Arimura Y, Nagaishi K, Isshiki H, Onodera K, Nakagaki S, Watanabe S, Idogawa M, Yamashita K, Naishiro Y, Adachi Y, Suzuki H, Fujimiya M, Imai K, Shinomura Y. | STEM CELLS | 2014 Apr. | 国外 |
| MicroRNA-31 expression in relation to BRAF mutation, CpG island methylation and colorectal continuum in serrated lesions. | Ito M, Mitsuhashi K, Igarashi H, Nosho K, Naito T, Yoshii S, Takahashi H, Fujita M, Sukawa Y, Yamamoto E, Takahashi T, Adachi Y, Nojima M, Sasaki Y, Tokino T, Baba Y, Maruyama R, Suzuki H, Imai K, Yamamoto H, Shinomura Y. | Int J Cancer | 2014 Apr. | 国外 |
| The effect of IGF-I receptor blockade for human esophageal squamous cell carcinoma and adenocarcinoma | Adachi Y, Ohashi H, Imsumran A, Yamamoto H, Matsunaga Y, Taniguchi H, Nosho K, Suzuki H, Sasaki Y, Arimura Y, Carbone DP, Imai K, Shinomura Y. | Tumor Biol | 2014 Feb. | 国外 |
| The role of DNA methylation in the genetics and epigenetics of multiple myeloma. | Yasui H, Ishida T, Imai K. | Series: Cancer Etiology, Diagnosis and Treatments. | 2014 | 国外 |
| Analysis of DNA methylation in bowel lavage fluid for detection of colorectal cancer. | Harada T, Yamamoto E, Yamano H, Nojima M, Maruyama R, Kumegawa K, Ashida M, Yoshikawa K, Kimura T, Harada E, Takagi R, Tanaka Y, Aoki H, Nishizono M, Nakaoka M, Tuyada A, Niinuma T, Kai M, Shimoda K, Shinomura Y, Sugai T, Imai K, Suzuki H. | Cancer Prevention Research | 2014 Aug. | 国外 |

17

| Title | Authors | Journal | Date | |
|---|---|---|---|---|
| Overview and Future prospect of "Promotion plan for the platform of human resource development for cancer" | Imai K | Juntendo Medical Journal | 2014 May. | 国内 |
| Everyday clinical practice in IgG4-related dacryoadenitis and/or sialadentist: Result from the SMART database. | Yamamoto M, Yajima H, Takahashi H, Yokoyama Y, Ishigami K, Shimizu Y, Tabeya T, Suzuki C, Naishiro Y, Takano K, Yamashita K, Hashimoto M, Keira Y, Honda S, Abe T, Suzuki Y, Mukai M, Himi T, Hasegawa T, Imai K, Shinomura Y. | Modern Rheumatology | 2014 Aug. | 国外 |
| IGF2 differentially methylated region hypomethylation in relation to pathological and molecular features of serrated lesions. | Naito T, Nosho K, Ito M, Igarashi H, Mitsuhashi K, Yoshii S, Aoki H, Nomura M, Sukawa Y, Yamamoto E, Adachi Y, Takahashi H, Hosokawa M, Fujita M, Takenouchi T, Maruyama R, Suzuki H, Baba Y, Imai K, Yamamoto H, Ogino S, Shinomura Y. | World Journal of Gastroenterol | 2014 Aug. | 国外 |
| CCAAT/enhancer binding protein α (C/EBP α )+ M2 macrophages contribute to fibrosis in IgG4-related disease? | Yamamoto M, Shimizu Y, Takahashi H, Yajima H, Yokoyama Y, Ishigami K, Tabeya T, Suzuki C, Matsui M, Naishiro Y, Imai K, Shinomura Y. | Mod Rheumatol | 2014 Sep. | 国外 |
| DNA synthesis inhibitors for the treatment of gastrointestinal cancer. | Yasui H, Tsurita G, Imai K. | Expert Opin Pharmacother. | Epub 2014 Sep. | 国外 |
| The Use of Bone Marrow Stromal Cells (Bone Marrow-Derived Multipotent Mesenchymal Stromal Cells) for Alveolar Bone Tissue Engineering: Basic Science to Clinical Translation. | Kagami H, Agata H, Inoue M, Asahina I, Tojo A, Yamashita N, Imai K. | Tissue Engineering Part B: Reviews | 2014 Nov. | 国外 |
| Association of microRNA-31-5p with clinical efficacy of anti-EGFR therapy in patients with metastatic colorectal cancer. | Igarashi H, Kurihara H, Mitsuhashi K, Ito M, Okuda H, Kanno S, Naito T, Yoshii S, Takahashi H, Kusumi T, Hasegawa T, Sukawa Y, Adachi Y, Okita K, Hirata K, Imamura Y, Baba Y, Imai K, Suzuki H, Yamamoto H, Nosho K, Shinomura Y. | Annals of Surgical Oncology | 2014 Dec. | 国外 |
| Screening of drugs to treat 8p11 myeloproliferative syndrome using patient-derived induced pluripotent stem cells with fusion gene CEP110-FGFR1. | Yamamoto S, Otsu M, Matsuzaka E, Konishi C, Takagi H, Hanada S, Mochizuki S, Nakauchi H, Imai K, Tsuji K, Ebihara Y. | Plos One | 2015 in press | 国外 |
| Clinicopathological and molecular characteristics of serrated lesions in Japanese elderly patients. | Nosho K, Igarashi H, Ito M, Mitsuhashi K, Kurihara H, Kanno S, Yoshii S, Mikami M, Takahashi H, Kusumi T, Hosokawa M, Sukawa Y, Adachi Y, Hasegawa T, Okita K, Hirata K, Maruyama R, Suzuki H, Imai K, Yamamoto H, Shinomura Y. | Digestion | 2015 Jan. | 国外 |
| Identification of relapse predictors in IgG4-related disease using multivariate analysis of clinical data at the first visit and initial treatment. | Yamamoto M, Nojima M, Takahashi H, Yokoyama Y, Ishigami K, Yajima H, Shimizu Y, Tabeya T, Matsui M, Suzuki C, Naishiro Y, Takano KI, Himi T, Imai K, Shinomura Y. | Rheumatology | 2015 Jan. | 国外 |
| Seasonal allergies and serial changes of serum levels of IgG4 in cases treated with maintenance therapy for IgG4-related disease. | Yamamoto M, Takahashi H, Shimizu Y, Yajima H, Suzuki C, Naishiro Y, Imai K, Shinomura Y. | Modern Rheumatology | 2015 Jan. | 国外 |
| Microsatellite instability. | Yamamoto H, Imai K. | Archives of Toxicology | 2015 in press | 国外 |

| | | | | |
|---|---|---|---|---|
| Association of Fusobacterium species in pancreatic cancer tissues with molecular features and prognosis. | Mitsuhashi K, Nosho K, Sukawa Y, Matsunaga Y, Ito M, Kurihara H, Kanno S, Igarashi H, Naito T, Adachi Y, Tachibana M, Tanuma T, Maguchi H, Shinohara T, Hasegawa T, Imamura M, Kimura Y, Hirata K, Maruyama R, Suzuki H, Imai K, Yamamoto H, Shinomura Y. | Oncotarget | 2015 in press | 国外 |
| Contextual niche signals towards colorectal tumor progression by mesenchymal stem cell in the mouse xenograft model. | Nakagaki S, Arimura Y, Nagaishi K, Isshiki H, Nasuno M, Watanabe S, Idogawa M, Yamashita K, Naishiro Y, Adachi Y, Suzuki H, Fujimiya M, Imai K, Shinomura Y. | J Gastroenterol | 2015 Feb. | 国外 |
| 総説 橋渡し研究の展開と我が国の医療 | 今井浩三 | 東京都病院薬剤師会雑誌 | 2014年4月 | 国内 |
| 人口動態に基づいた日本医療の未来予測 | 湯地晃一郎, 井元清哉, 山口類, 宮野悟, 上昌広, 今井浩三. | 南江堂臨床雑誌「外科」 | 2014年5月 | 国内 |
| 大規模コホートを用いた大腸癌のノンコーディングRNA発現異常と生活習慣の分子疫学的解析 | 能正勝彦, 五十嵐央祥, 伊藤美樹, 三橋 慧, 栗原弘義, 菅野伸一, 内藤崇史, 須河安恭敬, 松永康孝, 足立靖, 野島正寛, 今井浩三, 丸山玲緒, 鈴木 拓, 山本博幸, 篠村恭久 | 日本癌病態治療研究会誌 | 2014年6月 | 国内 |
| 総説 私とリウマチ学 | 今井浩三 | 分子リウマチ治療 | 2014年10月 | 国内 |
| がんエピゲノム異常を理解し、応用し、そして制御するために | 鈴木拓, 今井浩三 | 実験医学 | 2014年12月 | 国内 |
| 抗体医薬 | 安井寛, 今井浩三 | PHARMA TECH JAPAN 臨時増刊「DDS研究30年」 | 2015年1月 | 国内 |
| 抗体治療 特集「DDSがもたらした新しい臨床の風景」 | 佐々木茂, 篠村恭久, 今井浩三 | Drug Delivery System | 2015年1月 | 国内 |

# 学 会 等 発 表 実 績

委託業務題目「新規バイオマーカーPRDM14による難治性乳がん・すい臓がんの診断法の開発」
機関名　国立がん研究センター研究所
（前佛　均）

１．学会等における口頭・ポスター発表

| 発表した成果（発表題目、口頭・ポスター発表の別） | 発表者氏名 | 発表した場所（学会等名） | 発表した時期 | 国内・外の別 |
|---|---|---|---|---|
| CYP2D6 Genotype and Response to Neoadjuvant Tamoxifen Therapy:<br>A Prospective Study in Japan（口頭） | 前佛　均 | 第73回日本癌学会年会シンポジウム　横浜 | 2014年9月 | 国内 |
| CYP2D6 genotype and response to neoadjuvant Tamoxifen therapy: a prospective study in Japan.（口頭） | 前佛　均 | 第59回人類遺伝学会　東京 | 2014年11月 | 国内 |

２．学会誌・雑誌等における論文掲載

| 掲載した論文（発表題目） | 発表者氏名 | 発表した場所（学会誌・雑誌等名） | 発表した時期 | 国内・外の別 |
|---|---|---|---|---|
| Pharmacogenomics toward personalized tamoxifen therapy for breast cancer. | Zembutsu H | Pharmacogenomics. | 2015 | 国外 |
| Lymph node shape in computed tomography imaging as a predictor for axillary lymph node metastasis in patients with breast cancer. | Kutomi G, Ohmura T, Satomi F, Takamaru T, Shima H, Suzuki Y, Otokozawa S, Zembutsu H, Mori M, Hirata K. | Exp Ther Med | 2014 | 国外 |
| VAV3 mediates resistance to breast cancer endocrine therapy | Aguilar H, Urruticoechea A, Halonen P, Kiyotani K, Mushiroda T, Barril X, Serra-Musach J, Islam A, Caizzi L, Di Croce L, Nevedomskaya E, Zwart W, Bostner J, Karlsson E, Pérez Tenorio G, Fornander T, Sgroi DC, Garcia-Mata R, Jansen MP, García N, Bonifaci N, Climent F, Soler MT, Rodríguez-Vida A, Gil M, Brunet J, Martrat G, Gómez-Baldó L, Extremera AI, Figueras A, Balart J, Clarke R, Burnstein KL, Carlson KE, Katzenellenbogen JA, Vizoso M, Esteller M, Villanueva A, Rodríguez-Peña AB, Bustelo XR, Nakamura Y, Zembutsu H, Stål O, Beijersbergen RL, Pujana MA. | Breast Cancer Res | 2014 | 国外 |
| Polygenic inheritance of paclitaxel-induced sensory peripheral neuropathy driven by axon outgrowth gene sets in CALGB 40101 (Alliance). | Chhibber A, Mefford J, Stahl EA, Pendergrass SA, Baldwin RM, Owzar K, Li M, Winer EP, Hudis CA, Zembutsu H, Kubo M, Nakamura Y, McLeod HL, Ratain MJ, Shulman LN, Ritchie MD, Plenge RM, Witte JS, Kroetz DL. | Pharmacogenomics J | 2014 | 国外 |

| | | | | |
|---|---|---|---|---|
| CYP2D6 genotype and adjuvant tamoxifen: meta-analysis of heterogeneous study populations. | Province MA, Goetz MP, Brauch H, Flockhart DA, Hebert JM, Whaley R, Suman VJ, Schroth W, Winter S, Zembutsu H, Mushiroda T, Newman WG, Lee MT, Ambrosone CB, Beckmann MW, Choi JY, Dieudonné AS, Fasching PA, Ferraldeschi R, Gong L, Haschke-Becher E, Howell A, Jordan LB, Hamann U, Kiyotani K, Krippl P, Lambrechts D, Latif A, Langsenlehner U, Lorizio W, Neven P, Nguyen AT, Park BW, Purdie CA, Quinlan P, Renner W, Schmidt M, Schwab M, Shin JG, Stingl JC, Wegman P, Wingren S, Wu AH, Ziv E, Zirpoli G, Thompson AM, Jordan VC, Nakamura Y, Altman RB, Ames MM, Weinshilboum RM, Eichelbaum M, Ingle JN, Klein TE; International Tamoxifen Pharmacogenomics Consortium | Clin Pharmacol Ther. | 2014 | 国外 |
| Precision Medicine for Cancer and Pharmacogenomics | Zembutsu H. | 血液内科 | 2015 in press | 国内 |

学 会 等 発 表 実 績

委託業務題目「新規バイオマーカーPRDM14による難治性乳がん・すい臓がんの診断法の開発」

機関名　東京大学医科学研究所

（谷口博昭）

１．学会等における口頭・ポスター発表

| 発表した成果（発表題目、口頭・ポスター発表の別） | 発表者氏名 | 発表した場所（学会等名） | 発表した時期 | 国内・外の別 |
|---|---|---|---|---|
| ヒストンメチル化転移酵素PRDM14分子を標的とした核酸製剤による乳がん治療法の開発（口頭） | 谷口博昭、山本博幸、今井浩三 | 第73回日本癌学会学術総会 | 2014年10月 | 国内 |
| 乳がんを対象としたヒストンメチル基転移酵素を標的とする新規核酸製剤の開発(口頭) | 谷口博昭 | 文部科学省・次世代がんシーズ戦略的育成プログラム公開シンポジウム「革新的創薬シーズを活かす最先端DDS・イメージング技術」 | 2014年10月 | 国内 |
| 転写因子PRDM14分子を標的とした新規RNAi-ミセル複合体による乳がん治療法の開発(口頭) | 谷口博昭、前田芳周、宮田完二郎、山本博幸、片岡一則、今井浩三 | 第30回DDS学会 | 2014年7月 | 国内 |
| PRDM14 contribution to breast cancer progression and therapeutic model using PRDM14 RNAi (Oral) | 谷口博昭、山本博幸、越川直彦、今井浩三 | 第23回がん転移学会学術総会 | 2014年7月 | 国内 |
| Developing novel strategies for treatment on cancer metastasis (Oral) | 谷口博昭 | 第23回がん転移学会学術総会（第18回がん転移学会研究奨励賞受賞記念講演） | 2014年7月 | 国内 |

２．学会誌・雑誌等における論文掲載

| 掲載した論文（発表題目） | 発表者氏名 | 発表した場所（学会誌・雑誌等名） | 発表した時期 | 国内・外の別 |
|---|---|---|---|---|
| The effect of IGF-I receptor blockade for human esophageal squamous cell carcinoma and adenocarcinoma. | Adachi Y, Ohashi H, Imusumran A, Yamamoto H, Matsunaga Y, Taniguchi H , Nosho K, Suzuki H, Sasaki Y, ArimuraY, Carbone DP, Imai K, Shinoumura Y. | Tumor Biol, | 02/2014 | 国外 |
| An updated review of gastric cancer in the next-generation sequencing era: insights from bench to bedside and vice versa. | Yamamoto H, Watanabe Y, Maehata T, Morita R, Yoshida Y, Oikawa R, Ishigooka S, Ozawa S, Matsuo Y, Hosoya K, Yamashita M, Taniguchi H, Nosho K, Suzuki H, Yasuda H, Shinomura Y, Itoh F. | World J Gastroenterol. | 04/2014 | 国外 |

# Ⅳ．研究成果の刊行物・別刷

# Mesenchymal Stem Cells Cancel Azoxymethane-Induced Tumor Initiation

Masanao Nasuno,[a] Yoshiaki Arimura,[a] Kanna Nagaishi,[b] Hiroyuki Isshiki,[a] Kei Onodera,[a] Suguru Nakagaki,[a] Shuhei Watanabe,[a] Masashi Idogawa,[c] Kentaro Yamashita,[a] Yasuyoshi Naishiro,[d] Yasushi Adachi,[a] Hiromu Suzuki,[e] Mineko Fujimiya,[c] Kohzoh Imai,[f] Yasuhisa Shinomura[a]

[a]Department of Gastroenterology, Rheumatology, and Clinical Immunology, [b]Department of Anatomy, [c]Department of Medical Genome Sciences, Research Institute for Frontier Medicine, [d]Department of Educational Development, and [e]Department of Molecular Biology, Sapporo Medical University, Chuo-ku, Sapporo, Japan; [f]Center for Antibody and Vaccine Therapy, Institute of Medical Science, The University of Tokyo, Tokyo, Japan

Correspondence: Yoshiaki Arimura, M.D., Ph.D., Department of Gastroenterology, Rheumatology, and Clinical Immunology, Sapporo Medical University, S-1, W-16, Chuo-ku, Sapporo 060-8543, Japan. Telephone: +81-11-611-2111, Ext. 3211, 3213; Fax: +81-11-611-2282; e-mail: arimura@sapmed.ac.jp

## ABSTRACT

The role of mesenchymal stem cells (MSCs) in tumorigenesis remains controversial. Therefore, our goal was to determine whether exogenous MSCs possess intrinsic antineoplastic or proneoplastic properties in azoxymethane (AOM)-induced carcinogenesis. Three in vivo models were studied: an AOM/dextran sulfate sodium colitis-associated carcinoma model, an aberrant crypt foci model, and a model to assess the acute apoptotic response of a genotoxic carcinogen (AARGC). We also performed in vitro coculture experiments. As a result, we found that MSCs partially canceled AOM-induced tumor initiation but not tumor promotion. Moreover, MSCs inhibited the AARGC in colonic epithelial cells because of the removal of $O^6$-methylguanine ($O^6$MeG) adducts through $O^6$MeG-DNA methyltransferase activation. Furthermore, MSCs broadly affected the cell-cycle machinery, potentially leading to G1 arrest in vivo. Coculture of IEC-6 rat intestinal cells with MSCs not only arrested the cell cycle at the G1 phase, but also induced apoptosis. The anti-carcinogenetic properties of MSCs in vitro required transforming growth factor (TGF)-β signaling because such properties were completely abrogated by absorption of TGF-β under indirect coculture conditions. MSCs inhibited AOM-induced tumor initiation by preventing the initiating cells from sustaining DNA insults and subsequently inducing G1 arrest in the initiated cells that escaped from the AARGC. Furthermore, tumor initiation perturbed by MSCs might potentially dysregulate WNT and TGF-β-Smad signaling pathways in subsequent tumorigenesis. Obtaining a better understanding of MSC functions in colon carcinogenesis is essential before commencing the broader clinical application of promising MSC-based therapies for cancer-prone patients with inflammatory bowel disease. STEM CELLS 2014;32:913–925

## INTRODUCTION

Stem and progenitor cells are well-known direct cellular targets of genetic alterations in human carcinogenesis [1–3]. Previous studies have altered our perception of stromal cells from being innocent bystanders to active promoters in the neoplastic process [4–6]. Carcinoma formation accompanied by well-orchestrated desmoplastic reactions [7] closely resembles wound healing and scar formation, and entails the constant availability of growth factors, cytokines, and matrix-remodeling proteins that render the tumor site as a "wound that never heals" [8]. Recent studies have shown that bone marrow-derived mesenchymal stem cells (MSCs) are recruited in large numbers to the stroma of developing tumors [9, 10].

However, the role of MSCs in tumorigenesis remains an intensely debated topic. Khakoo et al. demonstrated that intravenously injected human MSCs possess intrinsic antineoplastic properties in an in vivo model of Kaposi's sarcoma by inhibition of Akt activity in a cell–cell contact-dependent manner [11]. In contrast, Karnoub et al. demonstrated that MSCs within the stroma of the tumor microenvironment facilitate metastatic spread via paracrine signals of C—C motif chemokine 5 that is secreted de novo by MSCs [12].

A meta-analysis of chemoprevention studies has suggested that azoxymethane (AOM)-based rodent models of carcinogenesis are valuable for prediction of chemopreventive efficacy in humans, which is better than that of other models [13, 14]. The prominent advantages of the AOM/dextran sulfate sodium (DSS) colitis-associated carcinogenesis model are that factors influencing tumor initiation [15, 16] should result in changes of the average tumor number per animal, whereas differences of the average tumor size typically provide evidence for factors involved in tumor

progression [17, 18]. AOM is a genotoxic agent that initiates cancer by alkylation of DNA, in which O6-methylguanine ($O^6$MeG) is a highly cytotoxic, apoptotic, mutagenic, recombinogenic, and clastogenic DNA adduct [19]. Conversely, dextran sulfate sodium (DSS) is not genotoxic, but rather a proinflammatory tumor promoter [20]. Studies in rodents have revealed that AOM-induced tumors resemble human colorectal cancer at the molecular level, which displays dysregulation of the canonical WNT signaling pathway, similar target genes [21–24], and mutation of K-ras [25].

Our goal was to determine whether MSCs possess intrinsic antineoplastic or proneoplastic properties in an AOM-induced tumorigenesis model. Because MSCs are prime candidates for use in cell- and gene-based therapies [26, 27], this essential information must be obtained before implementing the broader clinical application of MSC therapies.

## MATERIALS AND METHODS

For detailed Materials and Methods, refer to Supporting Information.

### Experimental Animals

Animal studies were performed under the supervision of the Committee for Animal Research of Sapporo Medical University in accordance with protocols approved by the Institutional Animal Care and Use Committee. All animals were maintained according to the guidelines of the Committee for Animal Research of Sapporo Medical University. Lewis rats were purchased from Charles River Laboratories Japan (Yokohama, Japan; http://www.crj.co.jp), and SD-TG (CAG-EGFP) rats were purchased from Japan SLC, Inc. (Hamamatsu, Japan; http://www.jslc.co.jp/) [28]. All rats were aged 6 weeks and were female unless indicated otherwise and were housed under pathogen-free conditions and received autoclaved food and water ad libitum.

### Cell Lines and Culture Conditions

Bone marrow cells were harvested by inserting a needle into the shaft of the femur or tibia and flushing it with 30 ml α-modified Eagle's medium (αMEM) containing 20% fetal bovine serum (FBS). To harvest rat MSCs [29], the cell suspensions were passed through a 70-μm nylon filter (Becton Dickinson, Franklin Lakes, NJ; http://www.bd.com/us/) and plated in 75-$cm^2$ flasks. Cells were grown in alpha-modified Eagle's medium (MEM) containing 20% FBS at 37°C and 5% $CO_2$. After 3 days, the medium was replaced with fresh αMEM containing 10% FBS, and the adherent cells were grown to 80% confluence to obtain passage 0. In accordance with the International Society for Cellular Therapy criteria [30], cells between passages 3 and 5 were used for subsequent experiments [26]. To harvest rat hematopoietic stem cells (HSCs) [31], CD90.1 (Thy1.1)$^+$ cells were magnetically labeled with CD90.1 MicroBeads (Miltenyi Biotec GmbH, Gladbach, Germany; https://www.miltenyibiotec.com/en/) for 15 minutes. Then, the cell suspension was loaded onto a MACS column that was placed in the magnetic field of a MACS separator. The magnetically labeled CD90.1$^+$ cells were retained and then eluted as the positively selected cell fraction. Detailed protocols and data sheets are available at http://www.

miltenyibiotec.com. To prepare conditioned medium from rat MSCs (MSC-CM), MSCs (4 × $10^5$ cells per 150-mm culture dish) were seeded and cultured to confluency. Then, the medium was changed to serum-free Dulbecco's modified Eagle's medium (Invitrogen, Carlsbad, CA; lifetechnologies. com), and the rat MSCs were cultured for a further 48 hours. The conditioned medium was collected, centrifuged at 300$g$ for 5 minutes, filtered using a 0.22-μm syringe filter, and then stored at −80°C until use.

IEC-6 cells obtained from the American Type Culture Collection (Manassas, VA; http://www.atcc.org/) and 3Y1 rat fibroblasts (3Y1-B Clone 1–6) [32] obtained from JCRB Cell Bank (Saito, Japan; http://cellbank.nibio.go.jp/) were maintained as recommended by the depositors.

### AOM/DSS Colitis-Associated Carcinoma Model and Evaluation of Tumor Growth

We adopted the two-stage colon tumor model that mimics colitis-driven tumor development as described by Tanaka et al. [33]. A total of 39 female Lew rats were divided into three groups (n = 13 each group): two treatment groups and one control group (Fig. 1). The control group designated as "MSC (−)" was administered a single intraperitoneal injection of AOM (15 mg/kg body weight; Sigma-Aldrich, St. Louis, MO; http://www.sigmaaldrich. com/united-states.html) and was not treated with MSCs. Starting at 1 week after injection, the animals received 2.5% DSS (molecular weight 9,000–20,000; Sigma-Aldrich) in drinking water for 7 days, and then received no further treatment for 18 weeks. The group designated as "MSC Day0" was intravenously administered 2 × $10^4$ MSCs/g body weight on day 0 when AOM was injected, and the group designated as "MSC Day9" was administered MSCs on day 9 following the AOM administration corresponding to day 2 after receiving DSS in drinking water. Evaluation of tumor growth in the AOM/DSS colitis-associated carcinoma model is described in Supporting Information.

### Analysis of Aberrant Crypts

Fifteen female Lew rats were divided into three groups (n = 5 each group): two treatment groups and one control group (Fig. 3). The control group designated as MSC (−) was administered two separate intraperitoneal injections of AOM (15 mg/kg body weight) at 7 days apart (Days 0 and 7) and was not treated with MSCs. No further treatment was performed for 3 weeks. The group designated as "MSC Day1" was intravenously administered 2 × $10^4$ MSCs/g body weight on day 1, which was 1-day before AOM was first injected, and the group designated as "MSC Day8" was administered MSCs on day 8 (1-day after the second AOM administration). The rats were killed at the end of the study (week 4) by transcardial perfusion with 4% paraformaldehyde in phosphate buffered saline (PBS). The colon was removed and cut open from the anus to the cecum along the longitudinal axis. We defined the rectum as the segment at 2 cm proximal to the anus, and divided the entire colon into three segments each measuring approximately 7 cm in length: the distal colon including the rectum and the middle and proximal colon. The colon was spread flat between sheets of filter paper and fixed in 10% buffered formalin. Then, the colon tissues were stained with 0.2% methylene blue in saline according to the procedure described by Bird [34] to observe aberrant crypts (ACs).
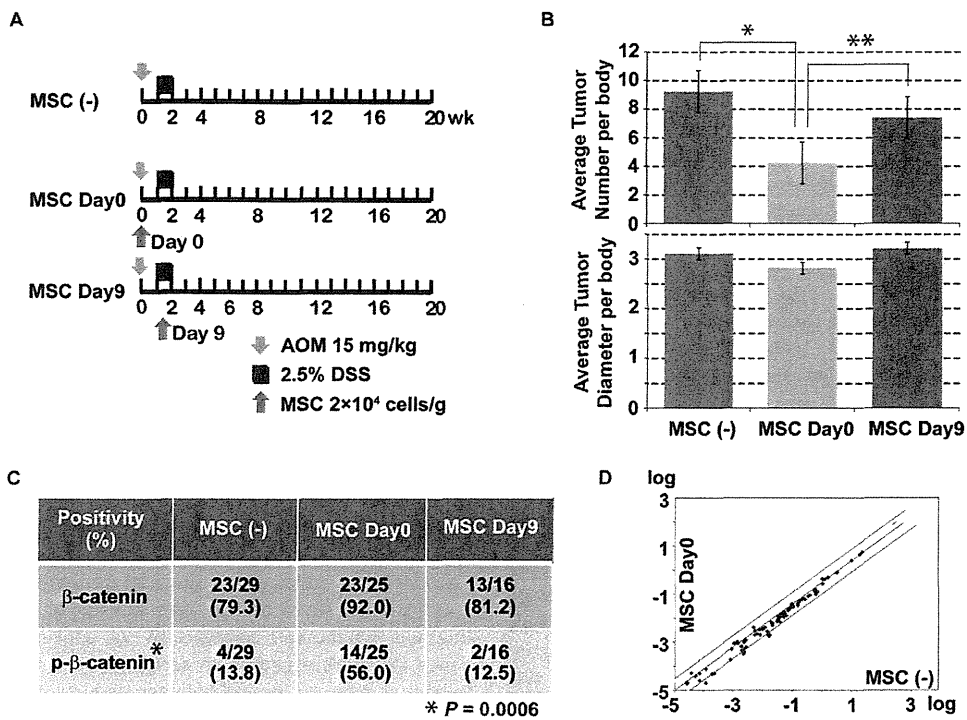
**Figure 1.** Effects of mesenchymal stem cells (MSCs) in the azoxymethane (AOM)/dextran sulfate sodium (DSS) colitis-associated carcinoma model. AOM/DSS model rats ($n = 39$) were classified into three groups ($n = 13$ each group) according to the timing of MSC administration in carcinogenetic phases: MSC-untreated control (MSC [−]), tumor initiation (day 0; MSC Day0), and tumor promotion phases (day 9; MSC Day9), as shown in panel A. Brown, orange, and blue bars represent data obtained from MSC (−), MSC Day0, and MSC Day9 groups, respectively. The upper panel of B shows the average tumor number per rat (a total of 271 tumors developed), and the lower panel indicates the average tumor size. *, $p = .023$; **, $p = .008$. The upper row of the panel C shows that $\beta$-catenin protein expression ($n = 70$ tumor tissues) was regarded as positive when the band intensity was stronger than that in the normal colon in Western blot analyses. In all, 23 of 29 (79.3%), 23 of 25 (92.0%), and 13 of 16 (81.2%) tumors examined were positive for $\beta$-catenin expression in MSC (−), MSC Day0, and MSC Day9 groups, respectively. The lower row indicates positivity of phospho-$\beta$-catenin at Ser33/37/Thr41 in Western blot analyses in the three groups. The contingency table analysis reached statistical significance (*, $p = .0006$). The WNT signal pathway polymerase chain reaction (PCR) array of representative samples pairs obtained from MSC (−) and MSC Day0 groups was depicted in panel D. PCR and Western blot analyses were performed in triplicate unless specified otherwise. Abbreviations: AOM, azoxymethane; DSS, dextran sulfate sodium; MSC, mesenchymal stem cell.

Based on the McLellan and Bird [35] definition, aberrant crypts (ACs) were defined as those that (i) were larger than normal crypts, (ii) had an increased pericryptal space that separated them from normal crypts, (iii) had a thicker layer of epithelial cells that often stained darkly, and (iv) generally had oval rather than circular openings. The number of aberrant crypt foci (ACF) per colon, the number of ACs in each focus, and the location of each focus were determined by stereomicroscopy (Olympus, Tokyo, Japan; http://www.olympus.co.jp/jp/) at 40X magnification. The mucosa of the distal segments was scraped off and subjected to Western blot analysis.

### Effects of MSCs on the AARGC

The five experimental groups included the MSC-untreated control group administered PBS, the group designated as "MSC" administered MSCs, groups designated as "hematopoietic stem cells (HSCs)" and "3Y1" administered HSCs or 3Y1 rat fibroblasts, respectively, and the group designated as "MSC-conditioned medium (MSC-CM)" treated with MSC-CM at 24 hours before AOM administration. Each group consisted of five rats and received a single subcutaneous injection of AOM (15 mg/kg body weight) at 09:00 hours. The

rats were then killed by $CO_2$-induced narcosis at the indicated intervals from 8 to 48 hours. The entire colon was removed immediately, cut open, and flushed with ice-cold saline. Segments measuring 2 cm were taken from the rectal end of the distal portion. These segments were immediately fixed in 10% paraformaldehyde overnight at room temperature and then embedded in paraffin. The mucosa on the remaining segments was scraped off and subjected to subsequent analyses.

### $\beta$-Catenin Nucleotide Sequence

Sequencing was performed by the classical Sanger method [36].

### WNT Signaling Pathway PCR Array Analysis

A rat WNT signaling pathway $RT^2$ profiler polymerase chain reaction (PCR) array (SuperArray Bioscience, Frederick, MD; http://www.sabiosciences.com/) was performed according to the manufacturer's instructions.

### Analysis of the Cell Cycle and Apoptosis

The cell cycle was assessed by flow cytometry and Ki67 immunohistochemistry. The apoptotic cell fraction was

determined by terminal deoxynucleotidyl transferase-mediated dUTP nick-end labeling (TUNEL) reactions.

## Immunofluorescence of the DNA Adduct of $O^6MeG$

The level of DNA alkylation was analyzed by immunofluorescence of distal colon sections using an antibody specific for the DNA adduct of $O^6MeG$. Frozen sections (4 µm) were prepared, rehydrated, and incubated with 3% hydrogen peroxide in 50% ethanol for 15 minutes at room temperature. Antigen retrieval was carried out with a Retrieval Solution (DAKO, Carpinteria, CA; http://www.dako.com/) for 10 minutes at 105°C in an autoclave. RNase treatment (20 µl RNase A at 10 mg/ml and 5 µl RNase T at 10 U/ml in 1,000 µl PBS, pH 7.5) was carried out for 1 hour at 37°C, and then stopped by treatment with a 140-mmol/l sodium chloride (NaCl) solution for 5 minutes at 4°C. DNA unwinding was achieved by alkali treatment (1,500 µl of 70 mmol/l NaOH/140 mmol/l NaCl and 1,000 µl of absolute methanol) before applying Protein Block (DAKO) for 10 minutes at room temperature. The sections were then incubated at room temperature overnight with an anti-$O^6MeG$ monoclonal antibody (clone EM 2–3; Squarix Biotechnology, Marl, Germany; http://www.squarix.de/) diluted at 1:1,000 in PBS. The next day, the sections were washed in PBS three times for 5 minutes each before applying an Alexa Fluor 594-labeled secondary anti-mouse IgG. Sections were counterstained with DAPI, dehydrated, and cover slipped for observation under a LSM 510 META. The primary antibody was omitted for the negative control.

## MTT Assay

Cell proliferation was measured by a MTT [3-(4,5-dimethylth-iazol-2-yl)-2,5-diphenyl-tetrazolium bromide] dye reduction assay [37].

## RNA Isolation and qPCR Analysis

Quantitative Real-Time PCR (qPCR) was performed using Taq-Man Universal PCR Master Mix (Applied Biosystems, Carlsbad, CA; lifetechnologies.com) for 40 cycles at 95°C for 15 seconds and 60°C for 1 minutes by standard methods.

## Western Blot Analysis

Western blot analysis was performed according to standard methods.

## MSC and IEC-6 Cell Coculture Experiments

Green fluorescent protein (GFP)-labeled rat MSCs were cocultured with the rat small intestinal cell line IEC-6. MSCs and IEC-6 cells cultured separately were included as controls. The cells were cocultured in RPMI 1,640 (Sigma-Aldrich) supplemented with 10% FBS, penicillin (100 U/ml), and streptomycin (100 µg/ml) at 37°C with 5% $CO_2$. A total of $1 \times 10^6$ MSCs were seeded per 100-mm dish for the MSC control and harvesting MSC-CM, and $1 \times 10^6$ IEC-6 cells per dish for the cell line control. For direct coculture, $1 \times 10^6$ MSCs per dish were preseeded for 2–3 hours. Then, $1 \times 10^6$ IEC-6 cells per dish were added and cultured for up to 72 hours with/without AOM treatment. For indirect coculture, 1,250 IEC-6 cells per well were preseeded in the lower chamber of a Transwell (0.4-µm pores, 48 wells; Corning, Tewksbury, MA; http://www.

corning.com) for 2–3 hours. Then, the same number of MSCs per well were added to the upper chamber of the Transwell and cultured for up to 72 hours with/without AOM, methylazoxymethanol (MAM; Wako Pure Chemical Industries, Tokyo, Japan; http://www.wako-chem. co.jp/), or $O^6$-benzylguanine ($O^6BG$; Sigma-Aldrich), which binds irreversibly to and inhibits the DNA repair enzyme $O^6MeG$-DNA methyltransferase (Mgmt). Because AOM is metabolized into the active metabolite methylazoxymethanol (MAM) by Cyp2e1, we confirmed whether Cyp2e1 was expressed in IEC-6 cells [38]. For absorption of transforming growth factor (TGF)-$\beta$, 1.0 µg/ml anti-transforming growth factor (TGF)-$\beta$ neutralizing antibody (Clone # 9016; R&D Systems, Minneapolis, MN; http://www.rndsystems.com/) was added to the direct coculture condition.

## Statistical Analysis

To compare means between two groups, parametric and non-parametric analyses were performed using the unpaired Student's $t$-test and the Mann–Whitney $U$-test, respectively. Categorical variables were compared using the chi-square test, exact $p$ value based on Pearson's statistic, or the Monte Carlo method. For multiple comparisons, we applied analysis of variance (ANOVA), especially in serial assessments, and two-way repeated measures (mixed between-within subjects) analysis of variance (ANOVA) followed by the Bonferroni test [39]. A difference was considered significant at $p < .05$ in all two-tailed tests. The SPSS Statistics 17.0 software package (SPSS Inc., Chicago, IL; http://www.spss.com/) was used for all statistical analyses.

## RESULTS

### MSCs Reduce the Tumor Number but Not the Tumor Size in AOM/DSS Colitis-Associated Tumorigenesis

We explored whether MSCs affected tumor initiation or promotion in the AOM/DSS model and the associated mechanism (Fig. 1A). The average tumor number per rat was significantly decreased by up to half of the expected level when MSCs were simultaneously injected with AOM (MSC Day0 group; $p = .008$ compared with the untreated control and $p = .023$ compared with the MSC Day9 group; upper panel in Fig. 1B and Supporting Information Fig. S1A). In contrast, the average tumor diameter was not significantly different among the groups as shown in the lower panel of Figure 1B. In this model, factors that influence tumor initiation should result in changes of the average tumor number per animal, whereas differences in average tumor sizes typically provide evidence of factors involved in tumor progression [18]. Therefore, these results suggest that MSC partially cancel AOM/DSS-induced tumor initiation.

### MSCs Profoundly Affect the Mutational Spectra During the Tumor Initiation Phase

As shown in Figure 1C, the tumor $\beta$-catenin expression analyzed by Western blotting was not significantly different among MSC (−), MSC Day0, and MSC Day9 groups. However, $\beta$-catenin was more frequently phosphorylated (56%, 14 of 25 tumors) in the MSC Day0 group than that in the MSC (−)
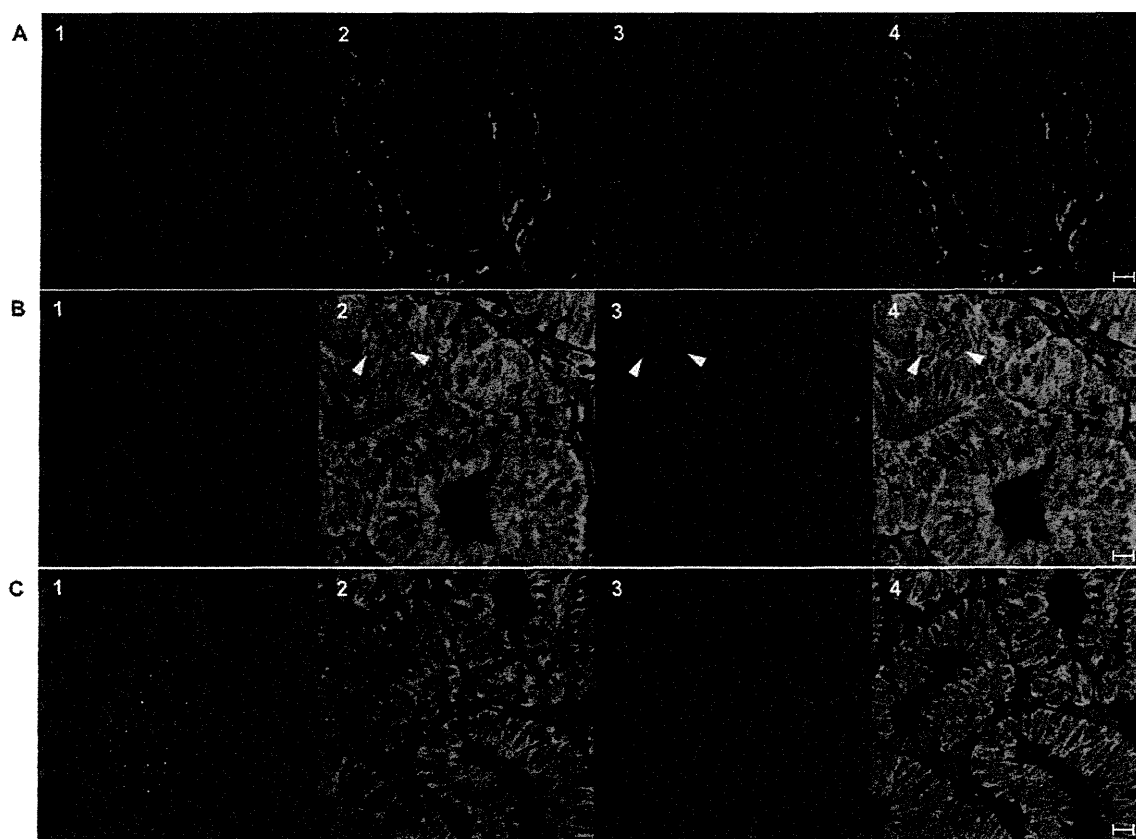
**Figure 2.** Double immunofluorescence staining of Smad2 and $\beta$-catenin. From the left to right, panels show nuclear counterstaining with DAPI (1), visualization of Smad2 (2) and $\beta$-catenin (3) using Alexa Fluor 488- and 594-labeled secondary antibodies, respectively, and merged images (4). Panel A shows normal colonic tissues of azoxymethane-untreated healthy rats, panel B shows tumor tissues from the mesenchymal stem cell (MSC) (−) group, and panel C shows tumor tissues from the MSC Day0 group. White arrowheads in panel B indicate nuclear staining of Smad2. Bar scales at the right lower corner in each panel indicated 10 μm.

group (13.8%, 4 of 29 tumors) and the MSC Day9 group (12.5%, 2 of 16, $p = .0006$). Furthermore, the mutation spectrum of $\beta$-catenin was quite different between MSC (−) and MSC Day0 groups. The codon 34 missense mutation (GGA–GAA) was the most frequent (11 of 25, 44%) in the MSC (−) group. In addition to the above mutation (5 of 15, 33.3%), the codon 32 missense mutation (GAT–AAT) was also frequently mutated (5 of 15, 33.3%) in the MSC Day0 group. Four (66.7%) of the six mutated regions detected in the MSC Day0 group and 12 (85.7%) of the 14 regions detected in the MSC (−) group appeared to be unique (Supporting Information Table S3). Of the 89 genes, 79 (88.8%) genes of the WNT signal pathway examined in the WNT PCR array were downregulated in MSC Day0 tumors compared with that in MSC (−) tumors (Fig. 1D).

Receptor-regulated Smad representing canonical TGF-$\beta$-Smad signaling was confined to the cell membrane of the laminar propria stromal cells, and $\beta$-catenin was expressed only on the cell membranes of crypt epithelial cells in the normal colon (Fig. 2A). Phospho-Smad2 expression representing activated TGF-$\beta$ signaling was not significantly different between MSC (−) and MSC Day0 groups in Western blot analyses (data not shown). The total Smad2 protein level was upregulated locally in the cytoplasm and partially in the nuclei (white arrowheads in Fig. 2B). $\beta$-Catenin was slightly upregu-

lated in membranous and cytoplasmic staining of the colon carcinomas in MSC (−) group rats (Fig. 2B). In contrast, both Smad2 and $\beta$-catenin were localized only on the membrane of colon carcinoma cells in MSC Day0 group rats (Fig. 2C). MSC engraftment was observed in tumors established at 20 weeks after AOM administration (data not shown). Therefore, these results suggest that MSCs profoundly affect the mutational spectra during the tumor initiation phase, leading to distinct WNT and canonical TGF-$\beta$-Smad signaling in subsequent tumorigenesis and even in the established tumors.

## MSCs Reduce the Formation of ACF

Next, we determined whether MSCs affect aberrant crypt foci (ACF) formation and the timing of MSC administration during tumor initiation induced by AOM for the most efficacious chemoprevention (Fig. 3A). The average ACF density was significantly lower in both pre-AOM (MSC Day−1; $p = 4.7E\text{-}4$) and post-AOM (MSC Day8; $p = .001$) treatment groups than that in the MSC (−) control group (Fig. 3B; Supporting Information Fig. S1B). As depicted in Figure 3C, ACF were formed more frequently in the distal colon than in the proximal colon as reported previously [34]. ACF formation was suppressed in both the distal and middle colons of both treatment groups (MSC Day1 and MSC Day8) with no significant differences between the two treatment groups. The multiplicity of ACs
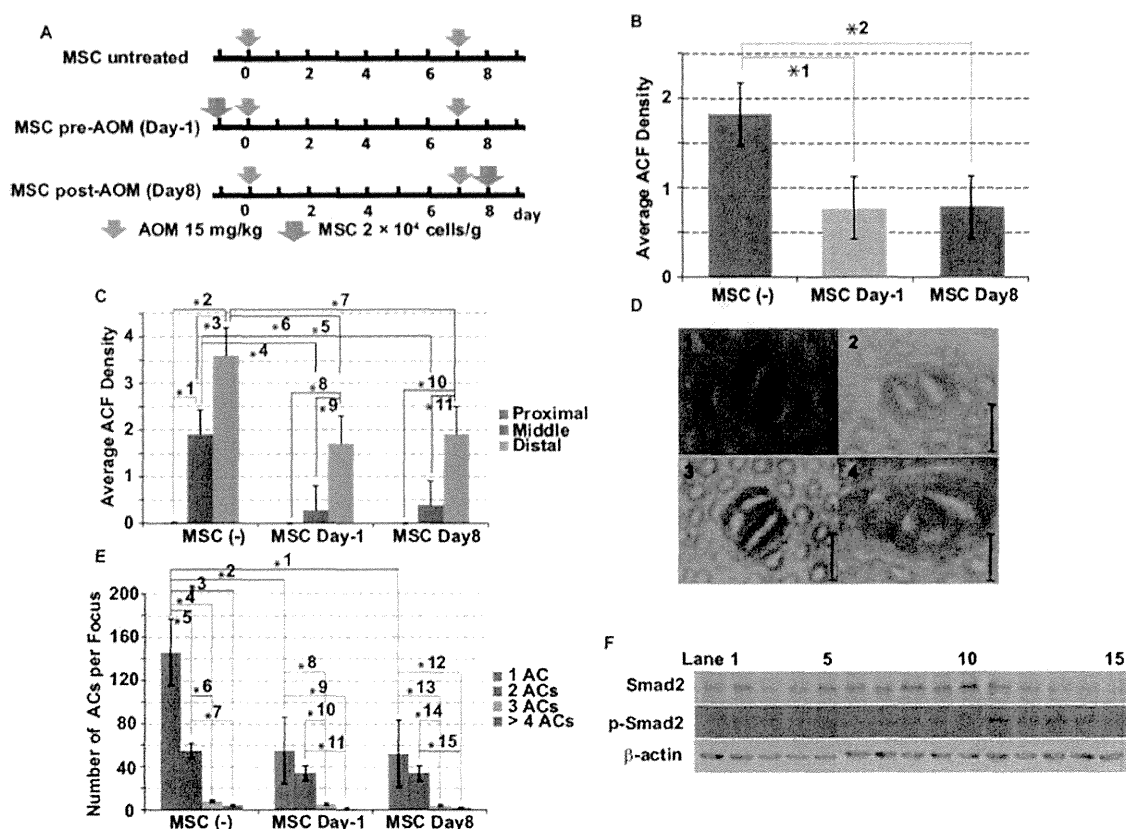
**Figure 3.** Analysis of the aberrant crypt foci (ACF) model. ACF model rats (*n* = 15) were classified into three groups (*n* = 5 each group) according to the timing of mesenchymal stem cell (MSC) administration either before or after administration of two separate of azoxymethane (AOM) on Days 0 and 7: MSC (−), MSC pre-AOM (Day−1), and MSC post-AOM (day 8) groups (A). A total of 400 ACF developed: 213, 95, and 92 in MSC (−), MSC Day−1, and MSC Day8 groups, respectively. The average ACF density is shown in panel B. *1, *p* = 4.7E-4; *2, *p* = .001. The average ACF density in the proximal, middle, and distal colon is shown in panel C. *1, *p* = .02; *2, *p* = 1.6E-4; *3, *p* = .037; *4, *p* = .017; *5, *p* = .022; *6, *p* = .002; *7, *p* = .004; *8, *p* = 4.0E-5; *9, *p* = 2.2E-4; *10, *p* = 2.1E-7; *11, *p* = 1.9E-6. Representative ACs, one to more than four ACs per focus, are shown in panels D1–4, respectively. Scale bars: 50 μm. The average density of ACs per focus, one to more than four ACs, is shown in panel E. *1, *p* = .009; *2, *p* = .011; *3, *p* = 5.2E-5; *4, *p* = 7.3E-5; *5, *p* = .005; *6, *p* = 7.3E-5; *7, *p* = 5.3E-5; *8, *p* = 1.7E-4; *9, *p* = 7.9E-5; *10, *p* = .021; *11, *p* = .005; *12, *p* = 4.0E-6; *13, *p* = 6.4E-6; *14, *p* = .001; *15, *p* = .001. Panel F shows the analysis of transforming growth factor-*β* signaling by Western blotting of Smad2 and phospho-Smad2. Lanes 1–5, 6–10, and 11–15 show data for MSC (−) control MSC Day–1, and MSC Day8 groups, respectively. Abbreviations: AC, aberrant crypt; ACF, aberrant crypt foci; AOM, azoxymethane; MSC, mesenchymal stem cell.

per focus, as shown in Figure 3D1 (one AC) to D4 (>four ACs), was reciprocally related to the frequency of the ACs. Among these ACs, one AC/focus was significantly reduced by MSC treatment, although there was no significant difference between the treatment groups (Fig. 3E). Canonical TGF-*β*-Smad signaling represented by phospho-Smad2 was activated in all colonic epithelia (5 of 5) of the MSC Day8 group and not in the colonic epithelia of MSC (−) or MSC Day−1 groups (Fig. 3F). Surprisingly, these results suggest that MSCs elicit a chemopreventive effect on formation of the prototype ACF (one AC/focus), both as a preventive measure in the preinitiation phase (MSC Day1) and a treatment measure in the post-initiation phase (MSC Day8). However, it is unknown why the canonical TGF-*β*-Smad signals were distinctly activated by the two measures.

## MSCs Suppress the AARGC

To obtain a further mechanistic insight into the antineoplastic properties of MSCs in AOM-induced carcinogenesis, we examined whether MSCs affect the acute apoptotic response of a

genotoxic carcinogen (AARGC) in vivo (Fig. 4A) [40]. The acute apoptotic response of a genotoxic carcinogen (AARGC) peaked at 8 hours after AOM administration, which was significantly suppressed only in the MSC-treated group compared with that in the MSC-untreated control, HSC, 3Y1, and MSC-CM groups (Fig. 4B, 4C). The Ki-67 labeling index of the colonic epithelia was significantly decreased at 24 and 48 hours only in the MSC group compared with that in the other groups (Fig. 4D, 4E). Western blot analyses revealed suppression of Akt in the AARGC (8 hour) observed in control groups was significantly activated in MSC groups, whereas activation of p38 in the AARGC observed in control groups was slightly suppressed in MSC groups (Fig. 4F). Consequently, these results suggest that AARGC suppression is a specific property of MSCs, which does not involve other cell types or humoral factors produced by MSCs. Because the AARGC is accepted as one of the in vivo mechanisms that suppress tumorigenicity, further experiments are necessity to explain why MSCs possess chemopreventive and AARGC suppression effects.

28
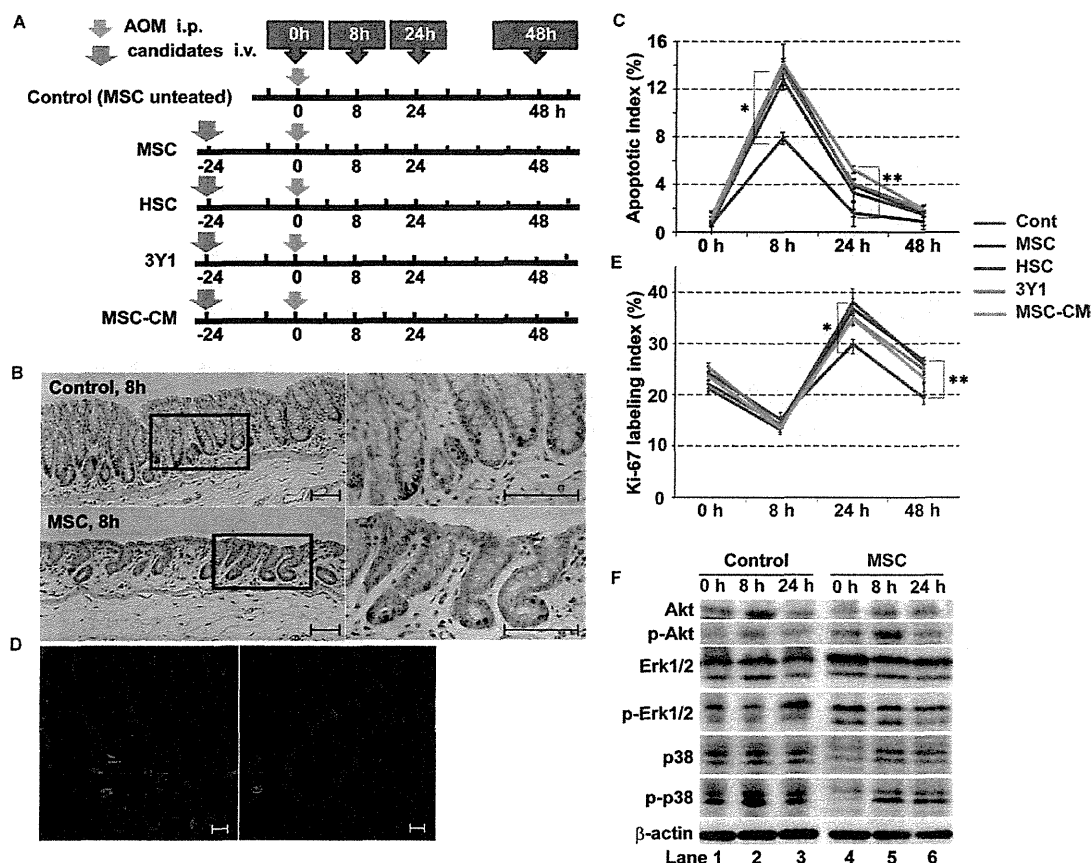
**Figure 4.** Effects of mesenchymal stem cells (MSCs) on the acute apoptotic response of a genotoxic carcinogen (AARGC). AARGC model rats ($n = 15$) were classified into five groups ($n = 5$ each group) according to the treatment at 24 hours before administration of a single dose of azoxymethane (AOM) on day 0: MSC ($-$) control (PBS), MSC, hematopoietic stem cell (HSC), 3Y1, and conditioned medium from rat MSC (MSC-CM) groups. Rats were killed at 0 hours when AOM was intraperitoneally injected at 4, 8, 16, 24, and 48 hours for subsequent analyses (A). Representative dUTP nick-end labeling (TUNEL) immunostaining is shown for control (upper) and MSC-24 hour groups (lower) at 8 hours. The right panel shows magnified views corresponding to the rectangles in the left panel (B). Bar scales at the right lower corner in each panel indicated 250 µm. The apoptotic index was calculated as the percentage of positive nuclear immuno-staining of TUNEL reactions in approximately 1,000 crypt epithelial cells at each indicated time point (C). *MSC versus control, $p = .006$; MSC versus HSC, $p = 2.9E\text{-}4$; MSC versus 3Y1, $p = .001$; MSC versus MSC-CM, $p = 1.7E\text{-}4$: **MSC versus HSC, $p = .010$; MSC versus 3Y1, $p = .005$; MSC versus MSC-CM $p = 1.3E\text{-}5$. Representative Ki-67 immunofluorescence is shown for control (left) and MSC groups (right) at 4 hours (D). Bar scales at the right lower corner in each panel indicated 10 µm. The Ki-67 labeling index was calculated as the per-centage of positive nuclear immunofluorescence in approximately 1,000 epithelial cells at each indicated time point (E). *MSC versus control, $p = .037$: **MSC versus control, $p = 2.2E\text{-}4$; MSC versus HSC, $p = 3.2E\text{-}5$; MSC versus 3Y1, $p = .002$. Ki-67 immunofluorescence and TUNEL reactions were performed using at least five different specimens in triplicate. Western blot analyses of Akt and mitogen-activated protein kinase (MAPK) signaling between MSC-treated and MSC-untreated control groups was performed (F). Abbreviations: ACF, aberrant crypt foci; AOM, azoxymethane; CM, conditioned medium; HSC, hematopoietic stem cell; MSC, mesenchymal stem cell.

## MSCs Reduces the Amount of DNA Adducts of $O^6$MeG

After administration, AOM is metabolized into MAM by Cyp2e1, which causes a DNA adduct of genotoxic $O^6$MeG. The methyl moiety in $O^6$MeG is then enzymatically removed by Mgmt. Therefore, we examined whether MSCs affect the level of $O^6$MeG using the above model to assess the AARGC in vivo. At 8 hours after AOM treatment, massive amounts of $O^6$MeG adducts were found in the colonic epithelia of MSC ($-$) control rats by $O^6$MeG immunofluorescence analysis (Fig. 5A). Furthermore, the amount of $O^6$MeG adducts was signifi-cantly reduced in the MSC-treated group (Fig. 5B). There were almost no positive signals for DNA adducts in healthy rats without AOM treatment at a basal physiological level (Fig. 5C). Moreover, at 8 hours after AOM exposure, the amount

of *Mgmt* transcripts was more abundant in MSC-treated groups than that in MSC-untreated control groups (Fig. 5D). These results suggest that MSCs indirectly remove $O^6$MeG adducts, likely though Mgmt activation.

## MSCs Profoundly Affect the Cell-Cycle Machinery

In Western blot analyses of the cell-cycle machinery (Fig. 5E), phospho-Smad2 was upregulated at 24 hours in the MSC-treated group. Expression of both I$\kappa$B$\alpha$ and p21 was gradually upregulated in the treated group, whereas it was gradually downregulated in the control group. Accordingly, *p21* expres-sion was upregulated at 4–8 hours in the MSC group as revealed by quantitative real-time PCR (qPCR) (data not shown). IKK phosphorylates NF$\kappa$B bound to I$\kappa$B$\alpha$, leading to
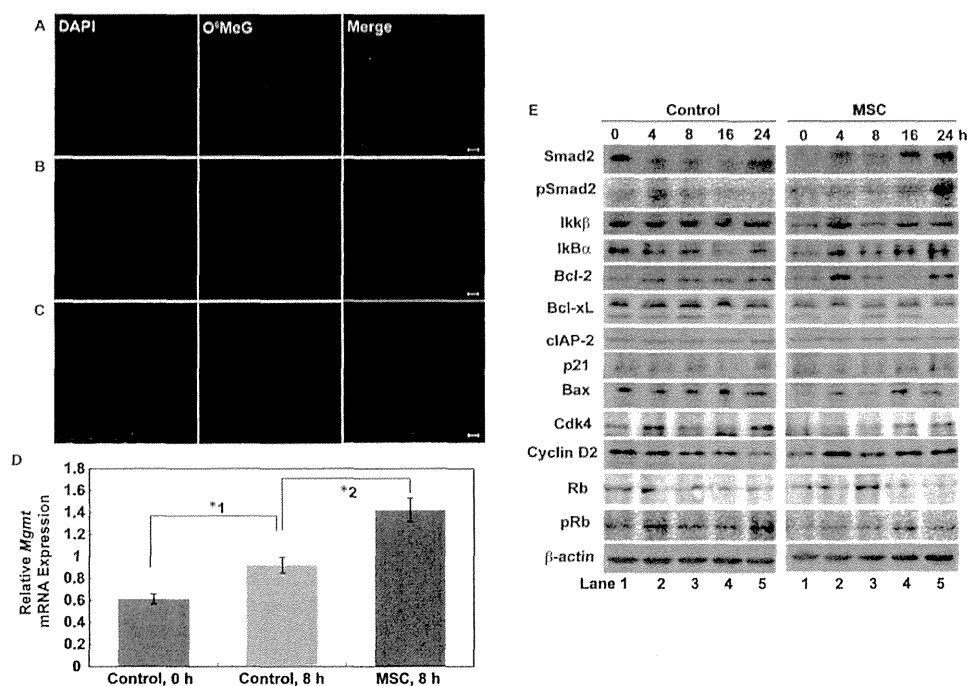
**Figure 5.** Mechanistic insight into the suppression of azoxymethane (AOM)-induced tumor initiation in vivo. The results of the in vivo immunofluorescence analysis of $O^6$MeG are depicted in panels **(A–C)**. The left panels show nuclei stained with DAPI, the middle panels visualize $O^6$MeG adducts in nuclear DNA using an Alexa Fluor 594-labeled secondary antibody, and the right panels are merged images of the left and middle panels in the same row. Panel **(A)** shows data from rats killed at 8 hours after AOM administration in the mesenchymal stem cell (MSC) (−) control group of the acute apoptotic response of a genotoxic carcinogen model, panel **(B)** shows data from rats killed at 8 hours after AOM administration in the MSC-24 hour group, and panel **(C)** shows data from AOM-untreated healthy rats. Bar scales at the right lower corner in each panel indicated 10 μm. In panel **(D)**, relative expression of *Mgmt* in the mucosa was evaluated by qualitative polymerase chain reaction. *1, $p = .021$; *2, $p = .018$. Panel **(E)** shows the results of Western blot analyses of Smad2, phospho-Smad2, IKK$\beta$, I$\kappa$B$\alpha$, Bcl-2, Bcl-xL, cIAP-2, p21, Bax, Cdk4, Rb, and phospho-Rb. Lanes 1–5 correspond to 0–24 hours, and the left and right panels correspond to the control and MSC-24 hour groups, respectively. The data are representative of three independent experiments. Abbreviations: DAPI, 4,6-diamidino-2-phenylindole; MSC, mesenchymal stem cell.

degradation of I$\kappa$B$\alpha$ and allowing NF-$\kappa$B signal activation. p21 Waf1/Cip1 are members of the Cip/Kip family of cyclin-dependent kinase (Cdk) inhibitors, which form heterotrimeric complexes with cyclins and Cdks, inhibiting kinase activity and blocking progression through G1/S-phase. Expression of Bax, a proapoptotic protein belonging to the Bcl-2 family, was slightly reduced in the treated group. Cyclins induced by mitogenic stimuli form a complex with Cdks. Cyclin dependent kinase 4 (Cdk4) complexes, which sequentially phosphorylate the retinoblastoma protein (Rb), facilitate G1–S transition. Cdk4 and phospho-retinoblastoma protein (Rb) appeared to be downregulated in the treated group. Taken together, MSCs might induce G1 arrest in colon epithelia, even after the AARGC, partially through the canonical TGF-$\beta$-Smad signaling pathway.

## MSCs Induce G1 Arrest and/or Apoptosis in IEC-6 Cells Mediated by TGF-$\beta$ In Vitro

Intriguingly, MSC suppressed ACF tumorigenesis even in the post-initiation phase (Fig. 3). Furthermore, in the model assessed on the AARGC, MSCs inhibited the cell-cycle machinery of cells evading the AARGC (Fig. 5). These observations strongly suggest that there are additional chemopreventive mechanisms of MSC other than a reduction of mutation load with $O^6$MeG. To investigation further, we conducted the following coculture experiments under AOM exposure. $O^6$-benzylguanine ($O^6$BG)

irreversibly inhibits Mgmt that demethylates $O^6$MeG caused by MAM. Thus, before AOM treatment, we confirmed that Cyp2e1 was expressed in IEC-6 cells (data not shown) as previously reported [38]. AOM exposure maintained proliferation and suppressed apoptosis of IEC-6 cells without coculture (the first blue bar in Fig. 6A, 6B, 6F [red line]). In contrast, IEC-6 cells cocultured with MSCs always showed inhibition of cell proliferation and acceleration of apoptosis depending on the received mutation load. The mutation load corresponded to the level of $O^6$MeG adduct depending on both the concentration and exposure time of the active metabolite, MAM (Fig. 6A, 6B). AOM treatment represented a minimal mutation load, whereas MAM plus $O^6$BG treatment represented the maximal mutation load in this setting. IEC-6 cells cocultured with MSCs under AOM exposure for 72 hours exhibited a significant reduction of proliferative activity (the first blue and second red bar in Fig. 6A, 6C, 6D). Cell-cycle analysis by flow cytometry revealed that IEC-6 cells cocultured under AOM exposure developed G1 arrest after 72 hours (Fig. 6E). To obtain a mechanistic insight into these phenomena, MTT assays under AOM exposure were performed using IEC-6 cells, IEC-6 cells treated with MSC-CM, IEC-6 cells directly or indirectly cocultured with MSCs, and IEC-6 cells directly cocultured with MSCs under anti-TGF-$\beta$ antibody exposure (Fig. 6F). Because the cells in both direct and indirect coculture were able to retain antiproliferative properties, the
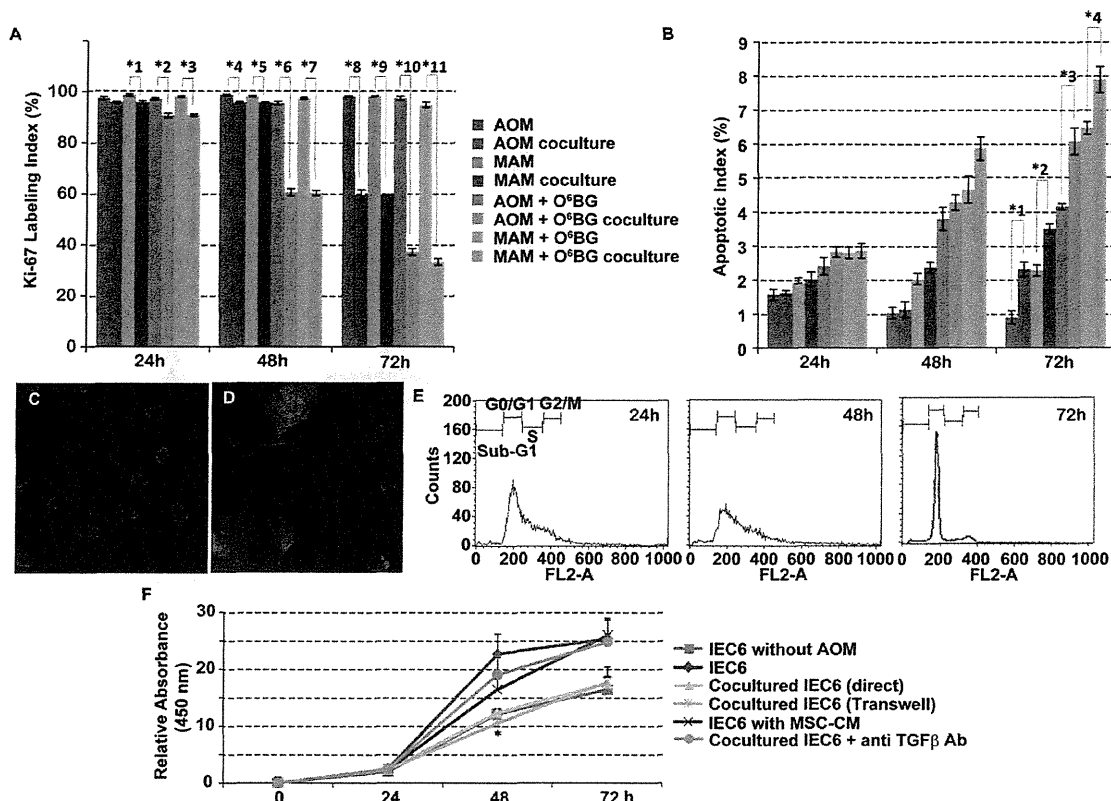
**Figure 6.** Mechanistic insight into suppression of azoxymethane (AOM)-induced tumor initiation in vitro. The Ki-67 labeling index was calculated in triplicate and bar charts were constructed for the following conditions: IEC-6 cells treated with AOM cocultured with or without mesenchymal stem cells (MSCs), IEC-6 cells treated with methylazoxymethanol (MAM) cocultured with or without MSCs, IEC-6 cells treated with AOM and $O^6BG$ cocultured with or without MSCs, and IEC-6 cells treated with MAM and $O^6BG$ cocultured with or without MSC **(A)**. *1, $p = 4.0E\text{-}4$; *2, $p = 4.0E\text{-}4$; *3, $p = 4.0E\text{-}4$; *4, $p = 4.0E\text{-}4$; *5, $p = 4.0E\text{-}4$; *6, $p = 4.0E\text{-}4$; *7, $p = 4.0E\text{-}4$; *8, $p = 4.0E\text{-}4$; *9, $p = 4.0E\text{-}4$; *10, $p = 4.0E\text{-}4$; *11, and $p = 4.0E\text{-}4$. The apoptotic index of IEC-6 cells was calculated based on dUTP nick-end labeling staining in triplicate and bar charts were constructed for the conditions described above **(B)**. Representative Ki-67 immunofluorescence of IEC-6 cells **(C)** and IEC-6 cell cocultures in which cells emitting green fluorescence are green fluorescent protein-labeled MSCs **(D)**. Cell culture images were taken at a magnifying power of 630. The cell cycle of cocultured IEC-6 cells was analyzed by flow cytometry at 24 hours (left), 48 hours (middle), and 72 hours (right) in triplicate **(E)**. IEC-6 proliferation was assayed by MTT for the following groups in triplicate: without AOM, cocultured with MSCs (direct), cocultured with MSCs (indirect), treated with conditioned medium from rat MSCs, and cocultured directly with MSCs and treated with anti-transforming growth factor-$\beta$ neutralizing antibodies **(F)**. Abbreviations: AOM, azoxymethane; CM, conditioned medium; IEC-6, the intestinal epithelioid cells, cell line No. 6; TGF-$\beta$, transforming growth factor-$\beta$; MAM, methylazoxymethanol.

humoral factors present under a direct heterotypic cell–cell interaction appeared to be important. This property of MSCs was completely abrogated by absorption of TGF-$\beta$ by neutralizing antibodies.

## DISCUSSION

### MSCs Exhibit Chemopreventive Properties by Primarily Canceling AOM-Induced Tumor Initiation

MSC administration led to a dramatic decrease of tumor incidence by up to half of the expected level without affecting the tumor size in the AOM/DSS colitis-associated carcinoma model (Fig. 1B). Consequently, our findings strongly suggest that MSCs exhibit chemopreventive properties by canceling AOM/DSS-induced tumor initiation. ACF, which are putative precursor lesions of colon tumors, represent alternative early end-points in AOM-induced colon carcinogenesis [34, 41, 42]. Although the early form of ACF, namely a single

AC per focus, was most frequently observed in our analysis, it was significantly decreased by MSC treatment independent of the timing of AOM administration (Fig. 3). This finding strongly suggests that MSCs do not reduce dysplastic ACF, but rather block ACF formation itself. This result motivated us to analyze the chemopreventive mechanisms exerted by MSCs as early as the AARGC in AOM-induced tumorigenesis.

### The AARGC Is Apparently Suppressed by MSC Administration

Because evasion of apoptosis is one of the hallmarks of cancer [16], induction of apoptosis during carcinogenesis is a critical step in chemoprevention. It is an accepted notion that the AARGC might regulate the mutational load in the colon or eliminate DNA-damaged cells that might otherwise progress to malignancy [43]. Therefore, most chemopreventive agents enhance the AARGC. Counterintuitively, in this study, the AARGC was seemingly suppressed by up to one third
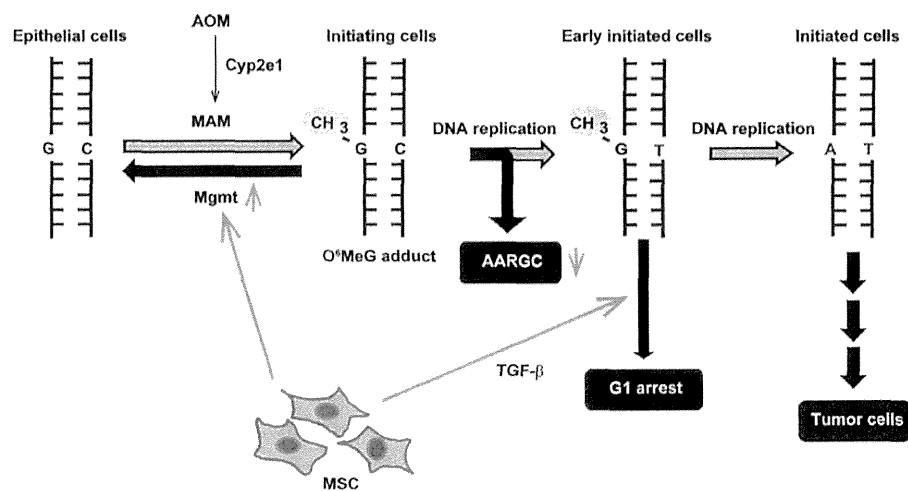
**Figure 7.** The tandem mechanisms of mesenchymal stem cell (MSC) chemoprevention involved in azoxymethane (AOM)-induced tumor initiation. The first mechanism of chemoprevention is an indirect measure exerted by MSCs: MSCs activate Mgmt in an unknown manner, resulting in suppression of the acute apoptotic response of a genotoxic carcinogen (AARGC) because of a reduction of initiating cells harboring $O^6$MeG adducts. The second mechanism is a direct measure: MSCs induce G1 arrest in early initiated cells evading the AARGC. Abbreviations: AOM, azoxymethane; MAM, methylazoxymethanol; MSC, mesenchymal stem cell; $O^6$MeG, O6-methylguanine; TGF-$\beta$, transforming growth factor-$\beta$.

following MSC treatment in the in vivo model compared with that in the MSC-untreated control (Fig. 4C). In contrast to our in vivo observations, in vitro experiments revealed that MSCs not only inhibited the proliferation of IEC-6 cells in coculture, but also accelerated apoptosis depending on the mutation load of the $O^6$MeG adduct level (Fig. 6). This discrepancy between in vitro and in vivo observations concerning apoptosis arises from investigations of the different phases of tumorigenesis between the two observations. MSCs can apparently prevent the AARGC in vivo because of pruning the DNA insults of $O^6$MeG adducts in the initiating cells, likely through Mgmt activation [44] or because of reducing production of the DNA adduct through Cyp2e1 inhibition [45]. These assumptions are directly supported by the immunofluorescence analysis showing that $O^6$MeG adducts were significantly decreased by MSC treatment. However, because MSCs upregulated Mgmt expression in the colonic mucosa of the AARGC model (Fig. 5D), the former pruning mechanism is more likely. In contrast to in vivo observations, increasing the mutation load of $O^6$MeG adducts using a combination of AOM or MAM with $O^6$BG linearly induced an increase of IEC-6 cell apoptosis in vitro (Fig. 6B). Cocultured MSCs directly augmented apoptosis caused by the mutation load of $O^6$MeG adducts in vitro, causing a discrepancy in the results regarding apoptosis between in vitro and in vivo observations. Our in vitro experiments examined the effects of MSCs on the survival of initiated cells beyond the AARGC, which corresponds more to the later phase of tumorigenesis than that in in vivo experiments. The detailed underlying mechanisms warrant further analyses.

## MSCs Induce $O^6$MeG-Triggered G1 Arrest and/or Apoptosis in the Initiated Cells Evading the AARGC

We determined whether cells that escape from the AARGC subsequently undergo G1 arrest or apoptosis in vivo. A reduction of ACF formation was observed by post-AOM treatment of MSCs representing initiated cells entering the postinitiation stage and pre-AOM treatment of MSCs representing cells that

remained at the preinitiation stage (Fig. 3A, 3B). Therefore, additional chemopreventive mechanisms appear to be exerted by MSCs other than a reduction of DNA insults. MSC-IEC-6 coculture experiments revealed that MSCs induced not only G1 arrest in IEC-6 cells, but also enhanced apoptosis depending on the mutational load received by AOM (Fig. 6A, 6B). These antineoplastic and proapoptotic properties of MSCs observed in vitro required TGF-$\beta$ signaling because they were completely abrogated by absorption of TGF-$\beta$ in cocultures (Fig. 6F). However, in contrast to the in vitro study, MSC treatment broadly affected the cell-cycle machinery to facilitate G1 arrest in colon epithelial cells in vivo (Fig. 5E). Moreover, it is unlikely that massive apoptosis occurs beyond the AARGC because the apoptotic index was distributed unimodally by steadily increasing and reaching a peak at the AARGC and then steadily decreasing for up to 48–72 hours (Fig. 4C). Apoptosis is caused by a series of complex responses involved in mismatch repair machineries and DNA double-strand breaks in subsequent consecutive and replicative cell cycles [46]. Consequently, a longer and closer observation is required to fully determine whether MSCs can induce $O^6$MeG-triggered apoptosis after evasion of the AARGC in vivo. In summary, MSCs reduce the number of initiating cells by pruning $O^6$MeG and/or inducing G1 arrest through TGF-$\beta$ signaling in early initiated cells (Fig. 7).

## Future Challenges for Better Understanding Chemopreventive Property of MSC

The mechanism of the first chemopreventive property of MSC, which was attributed to activation of Mgmt expression levels by MSCs, remains to be elucidated. MGMT expression is lost by epigenetic silencing in a variety of human cancers including nearly half of sporadic colorectal cancers [44]. On the other hands, similar to human colorectal cancer, AOM-induced tumors display global DNA hypomethylation. In addition, Mgmt is methylated in both AOM tumors and normal colon mucosa [47]. Collectively, these data suggest that epigenetic silencing of Mgmt by AOM

treatment can be abrogated by MSCs via unknown mechanisms. Thus far, at least three different layers have been elucidated for epigenetic regulation influencing the expression of MGMT: promoter methylation, histone modifications [48], and alternative polyadenylation with consecutive miRNA targeting [49]. Further studies are needed to confirm how MSCs cancel epigenetic silencing of Mgmt and which of the above regulatory mechanisms contribute to this process.

The level of cytosolic $\beta$-catenin is controlled by the so-called "$\beta$-catenin destruction complex" that facilitates casein kinase one alpha (CKI$\alpha$)- and GSK3 (glycogen synthase kinase)-mediated serial phosphorylation and subsequent polyubiquitination/degradation of $\beta$-catenin. However, missense $\beta$-catenin mutations at phosphorylation sites are known to prevent $\beta$-catenin degradation. In our study, we showed that MSCs facilitated $\beta$-catenin phosphorylation in the established tumors of the AOM/DSS model because MSCs induced a unique mutation spectrum of the $\beta$-catenin gene during the tumor initiation phase (Fig. 1C; Supporting Information Table S3). Degradation of phospho $\beta$-catenin is more likely to occur, which can lead to a reduction of Wnt signal activity. In support of this notion, the expression of most WNT signaling pathway molecules appeared to be suppressed in the tumors from MSC Day0 groups as shown by the WNT PCR array analysis (Fig. 1D). However, it largely remains to be clarified how alteration of the mutational spectra leads to a distinct sequela of tumor promotion and progression. The best-defined location of TGF-$\beta$/Wnt cross-talk is in the nucleus, where the Smad/$\beta$-catenin/lymphoid enhancer-bind (Lef) protein complex regulates numerous shared target genes, often in a synergistic manner. The implication of cooperative TGF-$\beta$ and Wnt signaling in tumor progression has recently been examined by Labbé et al. [50]. We demonstrated activation of both canonical pathways of TGF-$\beta$ and Wnt, whereas both pathways were suppressed by MSCs even in established tumors in which we could not detect any engrafted MSCs. Collectively, these findings suggest that MSCs appear to exert broader and more long-lasting so-called third mechanisms of chemoprevention, which extend beyond the tumor initiation phase in the AOM-induced tumorigenesis via regulation of the cross-talk between canonical Tgf-$\beta$ and Wnt signaling pathways than discussed heretofore.

Loss of canonical TGF-$\beta$-SMAD signaling is considered an essential step in carcinogenesis [51]. In fact, the activity of the Tgf-$\beta$ pathway is decreased by AOM treatment [52–54]. Tgf-$\beta$ expression has been found to be reduced in ACF [55, 56] but enhanced in colonic adenomas [55] and adenocarcinomas [57]. These observations suggest dual roles of Tgf-$\beta$ as an initial tumor suppressor and later as a tumor promoter in AOM-induced carcinogenesis as reported previously [58, 59]. Therefore, MSC activation of canonical Tgf-$\beta$-Smad signaling as a tumor suppressor only in the early initiated cells of the post-AOM MSC treatment group on day 8 in the ACF model (MSC Day8; Fig. 3F) suggests "the second"

chemopreventive mechanism of MSCs as discussed in detail earlier. Although canonical Tgf-$\beta$-Smad signaling was found to be activated in the established AOM/DSS tumors, Tgf-$\beta$ signal as a tumor promoter was inhibited in the tumor tissues from the MSC Day0 group (Fig. 2). This alteration of the signal probably reflects the whole integrated signals of a wide array of mutational events and likely does not reflect the effects of MSCs injected in the prior 20 weeks. However, it should be clarified whether this alteration of the Tgf-$\beta$ signal is related to the above "third" mechanisms of chemoprevention via the cross-talk between the canonical Tgf-$\beta$ and Wnt signaling pathway.

## CONCLUSION

Exogenous MSCs possess intrinsic antineoplastic properties against AOM-induced carcinogenesis. Although a complete mechanistic insight into the properties of MSCs has yet to be achieved, MSCs act as early as tumor initiation events either to reduce the number of initiating cells and/or to induce G1 arrest in early initiated cells (Fig. 7). Obtaining this information is essential before commencing the broader clinical application of promising MSC-based therapies for cancer patients, particularly cancer-prone patients with inflammatory bowel disease.

## AUTHOR CONTRIBUTIONS

M.N., K.O., S.N., and S.W.: acquisition, analysis, and interpretation of data; Y. Arimura: study concept and design, analysis and interpretation of data, drafting of the manuscript, and statistical analysis; K.N.: study concept and design, acquisition, analysis, and interpretation of data, and material support; H.I., M.I., K.Y., and Y. Adachi: critical revision of the manuscript for important intellectual content and analysis and interpretation of data; Y.N., and H.S.: analysis and interpretation of data and critical revision of the manuscript for important intellectual content; M.F.: technical and material support, and study supervision; K.I.: obtained funding and administrative support; Y.S.: study supervision and critical revision of the manuscript for important intellectual content.

## DISCLOSURE OF POTENTIAL CONFLICTS OF INTEREST

The authors indicate no potential conflicts of interest.

## REFERENCES

1  Scadden DT. Cancer stem cells refined. Nat Immunol 2004;5:701–703.

2  Reya T, Morrison SJ, Clarke MF et al. Stem cells, cancer, and cancer stem cells. Nature 2001;414:105–111.

3  Sell S. Stem cell origin of cancer and differentiation therapy. Crit Rev Oncol Hematol 2004;51:1–28.

4  Bhowmick NA, Neilson EG, Moses HL. Stromal fibroblasts in cancer initiation and progression. Nature 2004;432:332–337.

5  Bhowmick NA, Chytil A, Plieth D et al. TGF-beta signaling in fibroblasts modulates the oncogenic potential of adjacent epithelia. Science 2004;303:848–851.

6  Orimo A, Gupta PB, Sgroi DC et al. The influence of the microenvironment on the

malignant phenotype. Mol Med Today 200;6: 324–329.

7 Bissell MJ, Radisky D. Putting tumours in context. Nature Rev Cancer 2001;1:46–54.

8 Dvorak HF. Tumors: Wounds that do not heal. Similarities between tumor stroma generation and wound healing. N Engl J Med 1986;315:1650–1659.

9 Hall B, Andreeff M, Marini F. The participation of mesenchymal stem cells in tumor stroma formation and their application as targeted-gene delivery vehicles. Handb Exp Pharmacol 2007;180:263–283.

10 Ruan J, Ji J, Song H et al. Fluorescent magnetic nanoparticle-labeled mesenchymal stem cells for targeted imaging and hyperthermia therapy of in vivo gastric cancer. Nanoscale Res Lett 2012;7:309.

11 Khakoo AY, Pati S, Anderson SA et al. Human mesenchymal stem cells exert potent antitumorigenic effects in a model of Kaposi's sarcoma. J Exp Med 2006;203:1235–1247.

12 Karnoub AE, Dash AB, Vo AP et al. Mesenchymal stem cells within tumour stroma promote breast cancer metastasis. Nature 2007;449: 557–565.

13 Corpet DE, Pierre F. How good are rodent models of carcinogenesis in predicting efficacy in humans? A systematic review and meta-analysis of colon chemoprevention in rats, mice and men. Eur J Cancer 2005;41: 1911–1922.

14 Neufert C, Becker C, Neurath MF. An inducible mouse model of colon carcinogenesis for the analysis of sporadic and inflammation-driven tumor progression. Nat Prot 2007;2:1998–2004.

15 Fearon ER, Vogelstein B. A genetic model for colorectal tumorigenesis. Cell 1990;61:759–767.

16 Hanahan D, Weinberg RA. The hallmarks of cancer. Cell 2000;100:57–70.

17 Grivennikov SI, Greten FR, Karin M. Immunity, inflammation, and cancer. Cell 2010;140:883–899.

18 Greten FR, Eckmann L, Greten TF et al. IKKbeta links inflammation and tumorigenesis in a mouse model of colitis-associated cancer. Cell 2004;118:285–296.

19 Papanikolaou A, Shank RC, Delker DA et al. Initial levels of azoxymethane-induced DNA methyl adducts are not predictive of tumor susceptibility in inbred mice. Toxicol Appl Pharmacol 1998;150:196–203.

20 Bissahoyo A, Pearsall RS, Hanlon K et al. Azoxymethane is a genetic background-dependent colorectal tumor initiator and promoter in mice: Effects of dose, route, and diet. Toxicol Sci 2005;88:340–345.

21 Maltzman T, Whittington J, Driggers L et al. AOM-induced mouse colon tumors do not express full-length APC protein. Carcinogenesis 1997;18:2435–2439.

22 Takahashi M, Nakatsugi S, Sugimura T et al. Frequent mutations of the beta-catenin gene in mouse colon tumors induced by azoxymethane. Carcinogenesis 2000;21:1117–1120.

23 Guillem JG, Hsieh LL, O'Toole KM et al. Changes in expression of oncogenes and endogenous retroviral-like sequences during colon carcinogenesis. Cancer Res 1988;48: 3964–3971.

24 Wang QS, Papanikolaou A, Sabourin CL et al. Altered expression of cyclin D1 and cyclin-dependent kinase 4 in azoxymethane-induced mouse colon tumorigenesis. Carcinogenesis 1998;19:2001–2006.

25 Vivona AA, Shpitz B, Medline A et al. K-ras mutations in aberrant crypt foci, adenomas and adenocarcinomas during azoxymethane-induced colon carcinogenesis. Carcinogenesis 1993;14:1777–1781.

26 Yabana T, Arimura Y, Tanaka H et al. Enhancing epithelial engraftment of rat mesenchymal stem cells restores epithelial barrier integrity. J Pathol 2009;218:350–359.

27 Tanaka H, Arimura Y, Yabana T et al. Myogenic lineage differentiated mesenchymal stem cells enhance recovery from dextran sulfate sodium-induced colitis in the rat. J Gastroenterol 2011;46:143–152.

28 Hakamata Y, Tahara K, Uchida H et al. Green fluorescent protein-transgenic rat: A tool for organ transplantation research. Biochem Biophys Res Commun 2001;286:779–785.

29 Javazon EH, Colter DC, Schwarz EJ et al. Rat marrow stromal cells are more sensitive to plating density and expand more rapidly from single-cell-derived colonies than human marrow stromal cells. Stem Cells 2001;19: 219–225.

30 Dominici M, Le Blanc K, Mueller I et al. Minimal criteria for defining multipotent mesenchymal stromal cells: The International Society for Cellular Therapy position statement. Cytotherapy 2006;8:315–317.

31 Goldschneider I, Gordon LK, Morris RJ. Demonstration of Thy-1 antigen on pluripotent hemopoietie stem cells in the rat. J Exp Med 1978;1441:1351–1366.

32 Kimura G, Itagaki A, Summers J. Rat cell line 3y1 and its virogenic polyoma- and sv40-transformed derivatives. Int J Cancer 1975;15: 694–706.

33 Tanaka T, Kohno H, Suzuki R et al. A novel inflammation-related mouse colon carcinogenesis model induced by azoxymethane and dextran sodium sulfate. Cancer Sci 2003; 94:965–973.

34 Bird RP. Observation and quantification of aberrant crypts in the murine colon treated with a colon carcinogen: Preliminary findings. Cancer Lett 1987;37:147–151.

35 McLellan EA, Bird RP. Aberrant crypts: Potential preneoplastic lesions in the murine colon. Cancer Res 1988;48:6187–6192.

36 Sanger F, Nicklen S, Coulson AR. DNA sequencing with chain-terminating inhibitors. Proc Natl Acad Sci U S A 1977;12:5463–5467.

37 Sladowski D, Steer SJ, Clothier RH et al. An improved MTT assay. Immunol Methods 1993;157:203–207.

38 Sasaki T, Yoshida K, Shimura H et al. Inhibitory effect of linoleic acid on transformation of IEC6 intestinal cells by in vitro azoxymethane treatment. Int J Cancer 2006; 118:593–599.

39 Tabachnick BG, Fidell LS. Using Multivariate Statistics, Fifth Edition. Boston, MA: Pearson Education Inc., 2007:1–1008.

40 Hu Y, Martin J, Leu RL et al. The colonic response to genotoxic carcinogens in the rat: Regulation by dietary fibre. Carcinogenesis 2002;23:1131–1137.

41 Takayama T, Katsuki S, Takahashi Y et al. Aberrant crypt foci of the colon as precursors of adenoma and cancer. N Engl J Med 1998;339: 1277–1284.

42 Caderni G, Femia AP, Giannini A et al. Identification of mucin-depleted foci in the unsectioned colon of azoxymethane-treated rats: Correlation with carcinogenesis. Cancer Res 2003;63:2388–2392.

43 Le Leu RK, Brown IL, Hu Y et al. A synbiotic combination of resistant starch and Bifidobacterium lactis facilitates apoptotic deletion of carcinogen-damaged cells in rat colon. J Nutr 2005;135:996–1001.

44 Shen L, Kondo Y, Rosner GL et al. MGMT promoter methylation and field defect in sporadic colorectal cancer. J Natl Cancer Inst 2005;97:1330–1338.

45 Sohn OS, Fiala ES, Requeijo SP et al. Differential effects of CYP2E1 status on the metabolic activation of the colon carcinogens azoxymethane and methylazoxymethanol. Cancer Res 2001;61:8435–8440.

46 Quiros S, Roos WP, Kaina B. Processing of O6-methylguanine into DNA double-strand breaks requires two rounds of replication whereas apoptosis is also induced in subsequent cell cycles. Cell Cycle 2010;9:168–178.

47 Borinstein SC, Conerly M, Dzieciatkowski S et al. Aberrant DNA methylation occurs in colon neoplasms arising in the azoxymethane colon cancer model. Mol Carcinog 2010;49: 94–103.

48 Kitange GJ, Mladek AC, Carlson BL et al. Inhibition of histone deacetylation potentiates the evolution of acquired temozolomide resistance linked to MGMT upregulation in glioblastoma xenografts. Clin Cancer Res 2012;18:4070–4079.

49 Kreth S, Limbeck E, Hinske LC et al. In human glioblastomas transcript elongation by alternative polyadenylation and miRNA targeting is a potent mechanism of MGMT silencing. Acta Neuropathol 2013;125:671–681.

50 Labbé E, Lock L, Letamendia A et al. Transcriptional cooperation between the transforming growth factor-beta and Wnt pathways in mammary and intestinal tumorigenesis. Cancer Res 2007;67:75–84.

51 Derynck R, Akhurst RJ, Balmain A. TGF-$\beta$ signaling in tumor suppression and cancer progression. Nat Genet 2001;29:117–129.

52 Guda K, Claffey KP, Dong M et al. Defective processing of the transforming growth factor-beta1 in azoxymethane-induced mouse colon tumors. Mol Carcinog 2003;37:51–59.

53 Guda K, Giardina C, Nambiar P et al. Aberrant transforming growth factor-beta signaling in azoxymethane-induced mouse colon tumors. Mol Carcinog 2001;31:204–213.

54 Wang QS, Guda K, Papanikolaou A et al. Expression of transforming growth factor-beta1 and its type II receptor in mouse colon tumors induced by azoxymethane. Int J Oncol 2000;17:551–558.

55 Bird RP, Good CK. The significance of aberrant crypt foci in understanding the pathogenesis of colon cancer. Toxicol Lett 2000;112-113:395–402.

56 Thorup I. Histomorphological and immunohistochemical characterization of colonic aberrant crypt foci in rats: Relationship to

growth factor expression. Carcinogenesis 1997;18:465–472.

**57** Shao J, Sheng H, Aramandla R et al,. Coordinate regulation of cyclooxygenase-2 and TGF-$\beta$1 in replication error positive colon

cancer and azoxymethane-induced rat colonic tumors. Carcinogenesis 1999;20:185–191.

**58** Chen J, Huang XF. The signal pathways in azoxymethane-induced colon cancer and pre-

ventive implications. Cancer Biol Ther 2009;8: 1313–1317.

**59** Meulmeester E, ten Dijke P. The dynamic roles of TGF-$\beta$ in cancer. J Pathol 2011;223: 205–218.

See www.StemCells.com for supporting information available online.